Indian Journal of Chemical Technology
Vol. 31, March 2024, pp. 240-247
DOI: 10.56042/ijct.v31i2.3359

Photocatalytic treatment of N-Nitrosomorpholine by undoped TiO_2-ZnO & Si-doped TiO_2-ZnO nanocatalyst

J. Mary Juli Jenisha & G. Allen Gnana Raj*

Department of Chemistry & Research Centre Scott Christian College (Autonomous), Nagercoil-629003
(Affiliated to Manonmaniam Sundaranar University, Tirunelveli), Tamil Nadu, India

*E-mail: allengraj@gamil.com

Received 28 June 2023; accepted 12 January 2024

Photocatalytic degradation reactions of N-Nitrosomorpholine in an aqueous solution using nano anatase TiO_2-ZnO & Si-TiO_2-ZnO have been studied. The photocatalysts have been prepared by sol-gel method and characterised using SEM, EDX, XRD, FT-IR, UV, BET & TEM techinques. The loops seen in the BET study exhibited hysteresis following a type IV isotherm. The degradation process has been examined under various conditions including dark, induced light, UV light, direct sunlight, and sonicator in the presence of sunlight as the energy source. A decrease in band gap is observed for Si-TiO_2-ZnO as compared undoped TiO_2-ZnO, which results in improved photocatalytic activity in the doped sample. The Si-TiO_2-ZnO exhibited the highest level of photocatalytic activity when subjected to sonication in the presence of sunlight. The effects of several parameters, such as pH, pollutant concentration, and catalyst dose, the reaction rate etc. have been examined. Under optimal conditions, the pollutant underwent degradation and exhibited a degradation efficiency of 96% using Si-TiO_2-ZnO photocatalyst. The photocatalyst exhibits excellent stability when recycled for about four cycles. The remarkable efficiency of Si-TiO_2-ZnO under sunlight exposure highlights the extensive range of applications for photocatalysts in the removal of pollutants during water purification.

Keywords: Antifungal, N-Nitrosomorpholine degradation, Pollutant removal, Sol-gel method, Si-TiO_2-ZnO, TiO_2-ZnO

Introduction

The degradation of organically contaminants present in wastewater is a difficult task for any efficient photocatalyst. The expensive materials used in diverse processes result in non-biodegradable waste. In order to overcome these challenges, there is a need for a low-cost, non-toxic nanomaterial with superior photocatalytic abilities for dye degradation. Through mineralization, harmful organic pollutants may be photocatalyzed into less polluted byproducts with zero waste production[1]. The most common photocatalyst TiO_2 needs ultraviolet light to be activated. To increase the photocatalytic activity and create visible light sensitive catalysts, several changes to the structure and properties of TiO_2 have been proposed. Previous studies showed that the heterojunction of semiconductors with comparable band gaps, such as TiO_2 and ZnO, could have advantageous effects because the rate of recombination is reduced and the lifespan of the electron-hole pair is increased[2]. The crystallite size, specific surface area, morphologies, and textures of the semiconductor continue to have a significant impact on its photocatalytic capability[3]. Because of the interaction of photocatalysts with light to produce reactive hydroxyl or superoxide species, the degradation of organic pollutants can proceed more quickly.

Photocatalytic degradation is sometimes referred as the advanced oxidation process. It is applicable for the oxidation of a broad spectrum of organic molecules by harnessing light energy to disintegrate contaminants. This process involves the assimilation of photons within the visible, ultraviolet, and infrared electromagnetic spectra. The process of photocatalytic degradation starts with the production of charge carriers (e^-/h^+) by the absorption of light. The hole in the valence band undergoes oxidation of surface-absorbed water molecules or OH^-, resulting in the production of hydroxyl radicals ($^{\bullet}OH$). The essential process behind the photocatalytic destruction of contaminants by TiO_2 semiconductors is:

1. The stimulation of the semiconductor material to generate electron-hole pairs (EHP),
2. Generation of reactive oxygen species (ROS)
3. The subsequent breakdown of contaminants by ROS.

Semiconductor nanoparticles, including TiO_2 and ZnO, together with their nanocomposites have

exceptional photocatalytic activity in the breakdown of medicinal compounds. Despite the lack of direct causal evidence, a large group of chemical compounds known as nitrosamines have been classified as suspected human carcinogens[4-6]. N-Nitrosomorpholine (NMOR) is a cyclized nitrosamine. They are found in food, tobacco, and rubber and produced by the reaction of secondary amines with nitrite ions[7, 5]. In this paper Si-TiO_2-ZnO & TiO_2-ZnO were synthesised for the photocatalytic degradation of NMOR, which is a contaminant found in wastewater releasing from rubber and tyre industry.

Experimental Section

Tetra n-butyl ortho titanate ([$Ti(O\text{-}Bu)_4$]), zinc acetate (ZnAc), silicon tetrachloride ($SiCl_4$), ethanol & hydrochloric acid (HCl) with 99% purity were purchased from Sigma Aldrich.

Si-TiO_2-ZnO & TiO_2-ZnO were prepared by a sol-gel method. 50 mL of [$Ti(O\text{-}Bu)_4$], 50 mL of ethanol were taken in a 250 mL beaker and allowed to agitate for 30 min. In another beaker, 40 g of ZnAc, 40 mL of ethanol and 40 mL of distilled water were added and set to agitate for 30 min. 36 mL of 4.4 M HCl was added dropwise to the ZnAc solution and allowed to stir for 30 min. Titanium and zinc mixture were combined slowly under sonication. A white gel was formed, which was allowed to dry at 100 °C, powdered and calcined at 600 °C.

Similarly, Si-TiO_2-ZnO was prepared by adding 2 wt % of $SiCl_4$ with 50 mL of ethanol in 100 mL beaker and allowed to stir for 30 min. 50 mL of [$Ti(O\text{-}Bu)_4$] and 50 mL of ethanol were taken in a 250 mL beaker and allowed to agitate for 30 min. In another beaker, 40 g of ZnAc, 40 mL of ethanol and 40 mL of distilled water was added and set to agitate for 30 min. 36 mL of 4.4 M HCl was added dropwise to the ZnAc solution and allowed to stir for 30 min. All the solutions were combined under sonication, dried and calcined at 600 °C.

Results & Discussion

Characterisation of the catalyst

XRD analysis

XRD plot of the undoped TiO_2-ZnO as shown in Fig. 1a, the peaks at 32°, 35°, 48°, 53°, 56°, and 62° correspond to (100), (002), (200), (105), (110), and (213) planes, respectively. For Si-doped TiO_2-ZnO the peaks at 25°, 30°, 35°, 37°, 47°, 54°, and 62° correspond to (101, (100), (002), (004), (220), (105), and (213) planes, respectively. The planes (100), (002) and (110) in both undoped and doped TiO_2-ZnO can be assigned to wurtzite ZnO (JCPDS no. 36-1451). In both the figures, the planes (200), (105) and (213) can be assigned to tetragonal TiO_2 (JCPDS no. 21-1272) whereas in Fig. 3b, the planes (101), (004) and (220) can be assigned to cubic Si (JCPDS no. 89-2749).

FT-IR analysis

The photocatalysts were characterized by FT-IR spectroscopy for the confirmation of functional groups. In Fig. 2a the small band at 3775 cm^{-1} and 2365 cm^{-1} corresponds to O-H stretching, 2886 cm^{-1} for N-H stretching, 1612 cm^{-1} for C=C bending. The IR band of Ti-O-Ti is observed in the region 727 – 569 cm^{-1}. Below 1000 cm^{-1}, the peak shows the presence of Zn-O-H bonds. In Fig. 2b the broad band at 3563 cm^{-1} corresponds to O-H stretching, 2896 cm^{-1} to – N-H stretching, 1618 cm^{-1} to – C=C bending and the band in the region 741-600 cm^{-1} shows the presence of Si-O-Si, Ti-O-Ti and Zn-O-H bonds[8-12]. The weak peaks are due to the doping of Si to the semiconducting photocatalyst.

Band gap calculation (Tauc plot)

The band gaps of undoped and Si-doped TiO_2-ZnO were calculated by UV-visible absorption studies (Fig. 3a & 3b). From the absorption data the optical

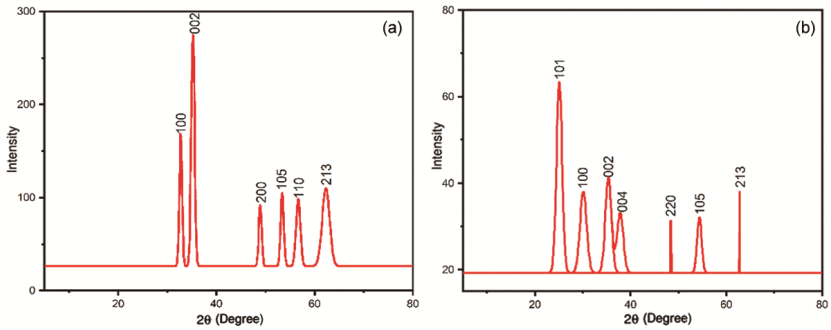

Fig. 1 — X-ray diffractograms of (a) undoped and (b) Si-doped TiO_2-ZnO photocatalyst

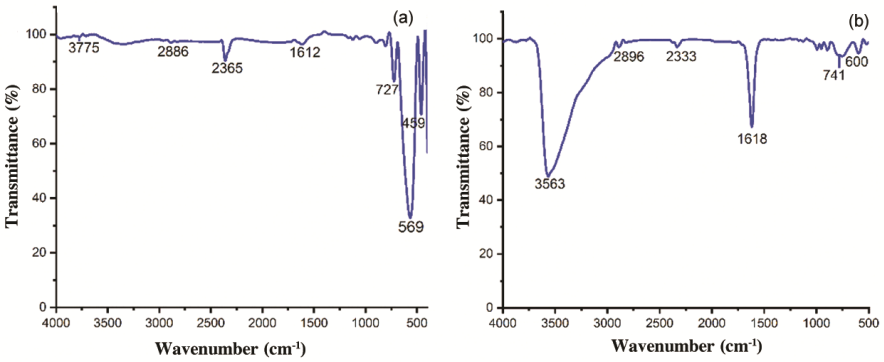

Fig. 2 — FT-IR spectra of (a) undoped TiO_2-Zn (b) Si-doped TiO_2-ZnO photocatalyst

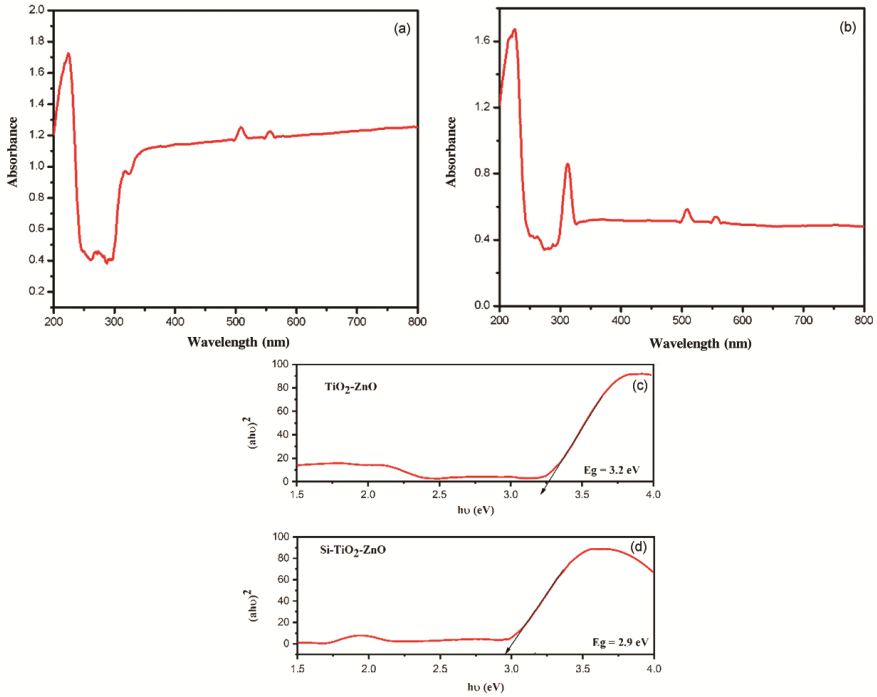

Fig. 3 —Absorption spectra of (a) undoped and (b) Si-doped TiO_2-ZnO with corresponding Tauc plots shown in (c) and (d), respectively

band gap was derived by plotting a Tauc relation plot, $(\alpha h\nu)^2 = A(h\nu\text{-}E_g)$, where a graph was plotted against the square root of absorption coefficient & photon energy (y-axis) versus photon energy (x-axis). The band gap of TiO_2-ZnO was found to be 3.2 eV and that of Si-TiO_2-ZnO was 2.9 eV (Fig. 3c). The band gap decreased upon doping in TiO_2-ZnO.

Microstructural analysis

The surface morphology was analysed by scanning electron microscopy (SEM) for TiO_2-ZnO and Si-TiO_2-ZnO photocatalysts. It analyses the dispersed electron from the surface of the particles, showing a semi-polygonal like shape for undoped TiO_2-ZnO and flaky-like appearance for Si-doped TiO_2-ZnO NPs as shown in Fig. 4a and 4b, respectively. The particles show aggregation with a lopsided distribution of shapes.

The elemental compositions were examined by the energy-dispersive X-ray spectroscopy (EDX) study. It shows 100% of elemental composition for both doped and undoped TiO_2-ZnO photocatalyst. Undoped TiO_2-ZnO demonstrates the existence of Ti, Zn, O & Cl as shown in Fig. 5a, whereas in Fig. 5b, Si- TiO_2-ZnO shows the presence of Si, Ti, Zn, O & Cl. Ti shows its presence at the peak of 4.5 & 4.9 keV, Zn at 1.2 & 8.6 keV, Si at 1.8 keV, Cl at 2.6 keV and O at 0.5 keV. Hence, the presence of elemental

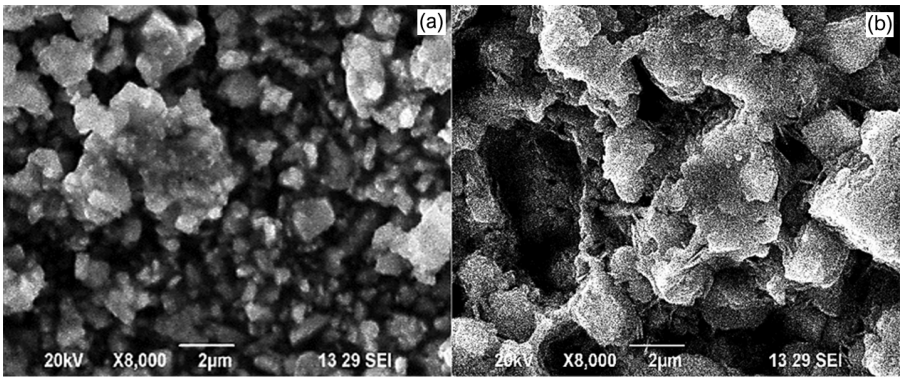

Fig. 4 — SEM image of (a) undoped and (b) Si-doped TiO_2-ZnO photocatalyst

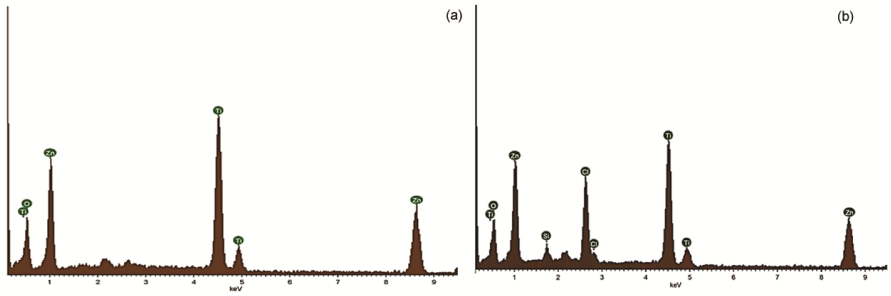

Fig. 5 — Elemental analysis of (a) undoped and (b) Si-doped TiO_2-ZnO photocatalyst

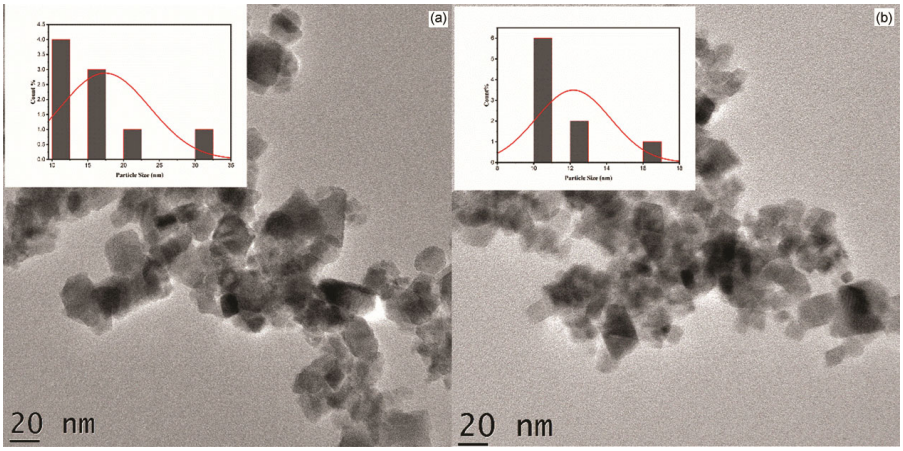

Fig. 6 — TEM images of (a) undoped and (b) Si-doped TiO_2-ZnO photocatalyst with Histogram and Gaussian fitting are given in the insets

composition confirms the synthesis of undoped TiO_2-ZnO & Si- TiO_2-ZnO.

Transmission electron microscopy (TEM) determines the morphology of the photocatalyst. The morphology is found to be semi-polygonal for both doped and undoped TiO_2-ZnO photocatalyst with uniform distribution of particles as shown in Fig. 6. The average particle size is determined by the histogram & Gaussian fitting data, which were resolved by the length measured from the TEM images as shown in the inset of respective figures. The average particle size of TiO_2-ZnO is 17.40 nm and for Si-doped TiO_2-ZnO is 12.17 nm.

BET analysis

For use of any nanomaterial as photocatalyst, the knowledge of its surface area is important which can be measured by Brunauer-Emmett-Teller (BET) technique. The adsorption/desorption isotherm and pore size distribution of TiO_2-ZnO and Si-TiO_2-ZnO is shown in Fig. 7(a-d). The surface area, pore volume & pore size is calculated and listed in Table.1.

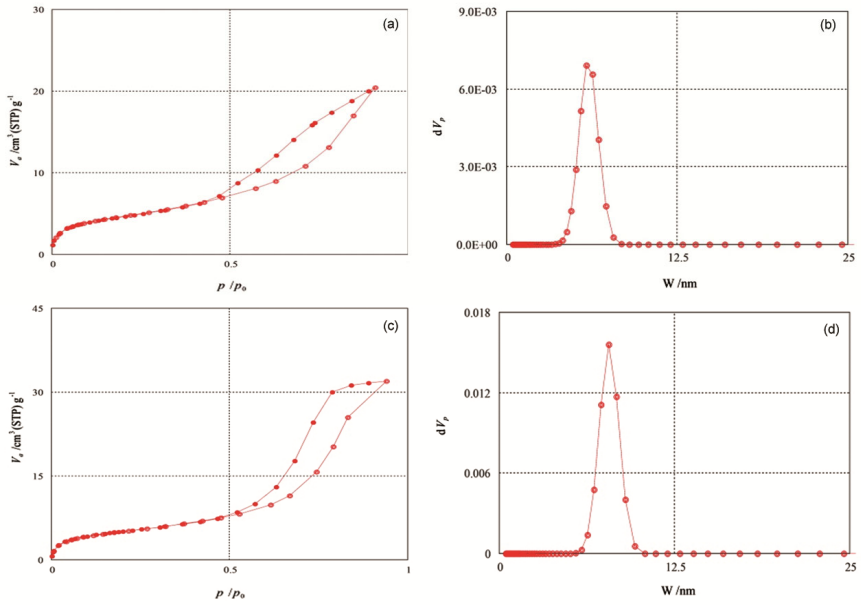

Fig. 7 — (a, c) Adsorption isotherm plot and (b, d) pore size analysis of undoped and Si-doped TiO_2-ZnO photocatalyst

Table. 1 — BET surface area analysis

Photocatalyst	BET surface area analysis		
	Surface area (m^2/g)	Pore volume (cm^3/g)	Pore size (nm)
TiO_2-ZnO	268.35	0.908	7.4677
Si-TiO_2-ZnO	402.86	0.941	10.688

In Fig. 7a and 7c the adsorption and desorption loops show type IV isotherm due to the hysteresis loop. The surface area of Si-doped TiO_2-ZnO is found to be higher than the undoped TiO_2-ZnO, which may be of the doping of Si to the photocatalyst. Usually, mesoporous silica shows high surface area.[13]

Photocatalytic degradation of NMOR

NMOR was employed as a model pollutant for photocatalytic degradation. NMOR absorbs at wavelength of 245 nm. It is subjected to degrade by undoped TiO_2-ZnO and Si-doped TiO_2-ZnO. The degradation was established under numerous parameters, as this plays a significant part in the deterioration process. The degradation percentage was calculated by the following equation:

Percentage degradation % = $(A_0\text{-}A)/ A_0*100$

Where, A_0 and A is the initial and final concentration of NMOR solution before after degradation, respectively.

Selection of different parameters

Different parameters play significant roles in the degradation process. They are as follows:

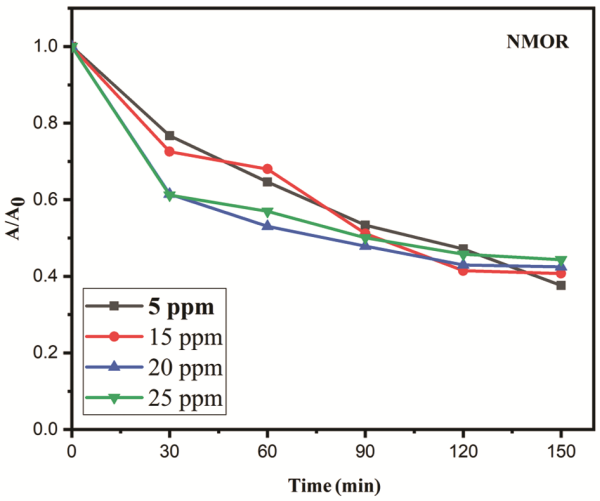

Fig. 8 — Impact of NMOR concentration on photocatalytic degradation of NMOR using TiO_2-ZnO photocatalyst

Impact of NMOR concentration

The impact of NMOR concentration on the photocatalytic degradation of NMOR using TiO_2-ZnO is depicted in Fig. 8. The effect of NMOR concentration on degradation was examined by varying the initial concentration of NMOR from 5 ppm to 25 ppm. When the concentration of NMOR was low, there were more active sites accessible on the surface of the catalyst, which coincided with an increase in the production of hydroxyl radicals. At high concentration, however, it demonstrated a lower efficiency due to the occurrence of multiple layers of adsorbed NMOR molecules on the surface of the catalyst. This, in turn,

inhibits the photoreaction. This is because there was no direct contact between the catalyst and photogenerated holes or hydroxyl radicals during the photocatalytic reaction. Furthermore, this prevents the substrate molecules from reaching the surface of the catalyst, which would have allowed them to adsorb light and photons [14-18]. It was observed that the photocatalytic effectiveness declines with increase in concentration due to a reduction in photon absorption on the photocatalyst because of the presence of more NMOR active sites. Therefore, at 5 ppm of substrate concentration and 0.02 g of TiO_2-ZnO photocatalyst NMOR substantially declines. Hence the concentration of NMOR was fixed to be 5 ppm for the following experiment.

Impact of pH

The impact of pH on the photocatalytic degradation of NMOR pollutant is depicted in Figs. 9(a) & (b). The pH range was adjusted to 4, 6 and 11. NMOR degrades effectively at pH 4 due to the protonation of holes. Furthermore, as the pH increases from acidic to alkaline medium the degradation efficiency decreases. This confirms that NMOR effectively degrades at pH 4.

Impact of light intensity

The impact of light intensity on the photocatalytic degradation of NMOR pollutants is depicted in Figs. 10a and 10b. The fact that NMOR exhibits no degradation in the dark suggests that NMOR is excited when exposed to light. Different light intensities, such as induced light, UV light, sunlight, and sunlight under sonication, were used to illustrate the degradation of NMOR pollutants. NMOR efficiently decay in the presence of sunlight under sonication, which exhibits the highest degradation when compared to other sources of light.

Photocatalytic degradation at optimum conditions

After evaluating the impact of each parameter, the optimum condition for best photocatalytic activity was chosen. A 5-ppm solution of NMOR was degraded using 0.02 g of TiO_2-ZnO under sunlight with constant sonication at frequency of 50-60 Hz and pH 4. For Si-TiO_2-ZnO, 0.06 g of the catalyst was used under the same condition. The degradation process was carried out by collecting the sample after 30 min intervals and observing the absorption wavelength. NMOR degrades at 150 min using TiO_2-ZnO & Si-TiO_2-ZnO photocatalyst. Where

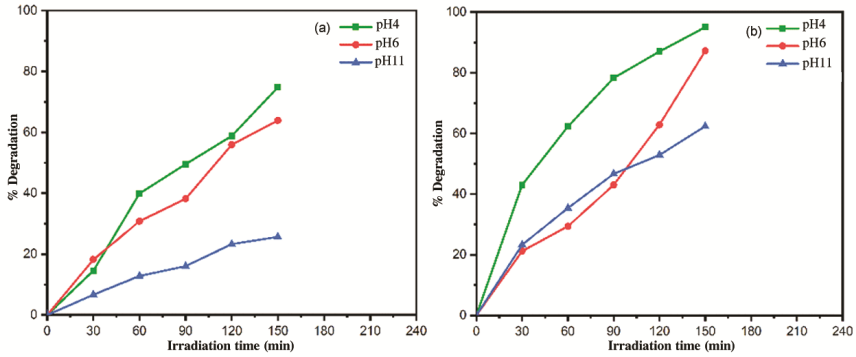

Fig. 9 — Impact of pH on photocatalytic degradation of NMOR using (a) undoped and (b) Si-doped TiO_2-ZnO photocatalyst

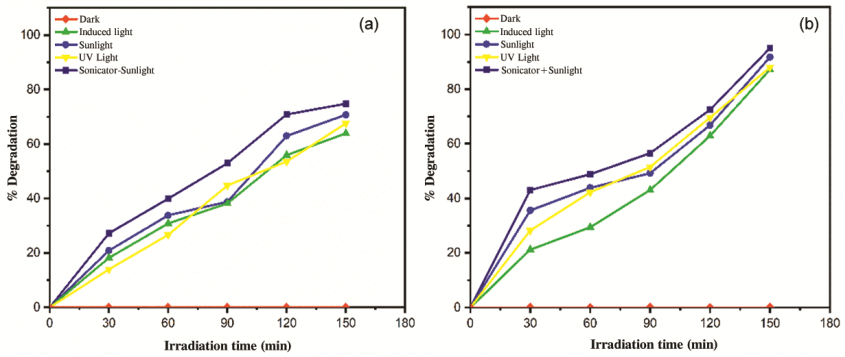

Fig. 10 — Impact of light intensity on photocatalytic degradation of NMOR using (a) undoped and (b) Si-doped TiO_2-ZnO photocatalyst

TiO_2-ZnO shows 75% (Fig. 11a) and 96% (Fig. 11b) degradation was observed for undoped and Si-doped TiO_2-ZnO, respectively. This concludes that doping narrows band gap and enhances the photocatalytic activity.

The kinetic model was plotted for the undoped TiO_2-ZnO & Si-doped TiO_2-ZnO photocatalyst at optimum condition in Fig. 12. It shows a linear plot against time (min) versus $\ln(A/A_0)$ which correlates to pseudo-first order kinetics. From the kinetic plot, the R^2 value for TiO_2-ZnO and Si-doped TiO_2-ZnO at optimum condition was calculated to be 0.9669 and 0.9792, respectively. The R_2 coefficient validates the strong connection between the empirical data and the model that has been adjusted.

Recycling of photocatalyst

The photocatalyst was reused by centrifuging the deteriorated solution, after which the residue was recovered, dried, and calcined. To assess the photocatalysts degrading effectiveness, it was recycled once again for about four cycles. The degradation efficiency indicates a gradual decline when the photocatalyst was reused as shown in Fig. 13. This confirmed that the photocatalysts TiO_2-ZnO and Si-TiO_2-ZnO have good stability with less than 20% decrease in their catalytic ability even after four cycles.

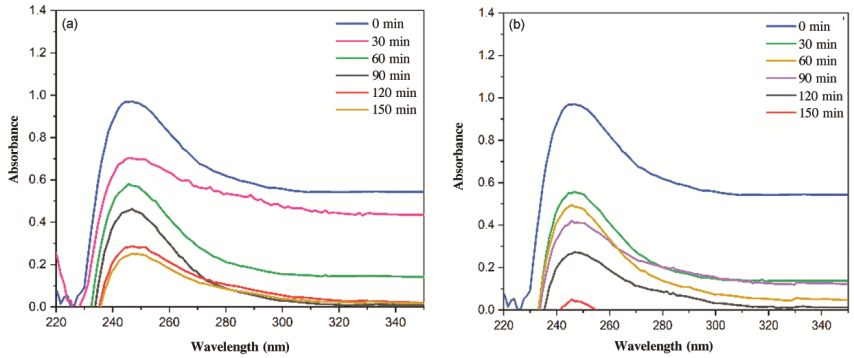

Fig. 11 — Photocatalytic degradation of NMOR using (a) undoped and (b) Si-doped TiO_2-ZnO photocatalyst

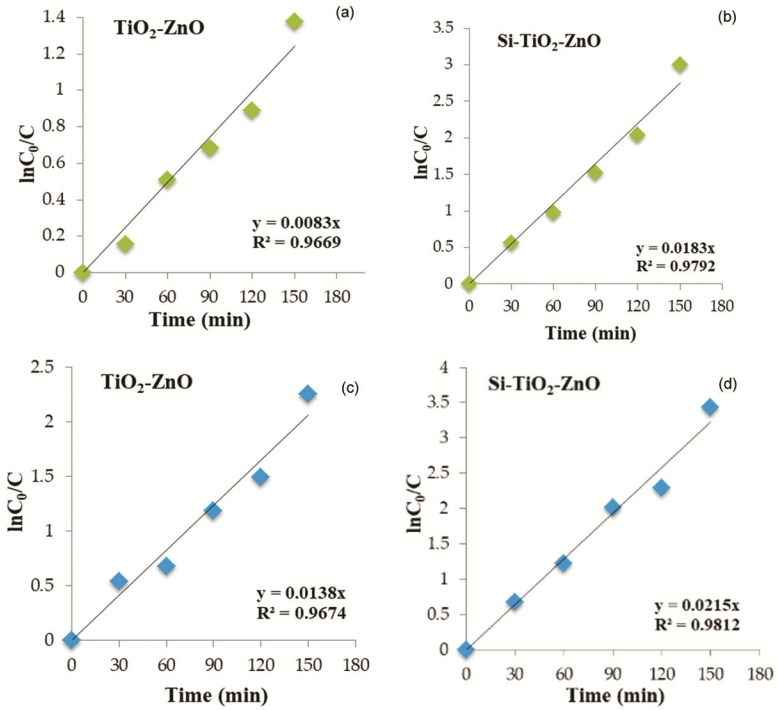

Fig. 12 — Kinetic study at optimum condition for (a,c) undoped and (b,d) Si-doped TiO_2-ZnO photocatalyst

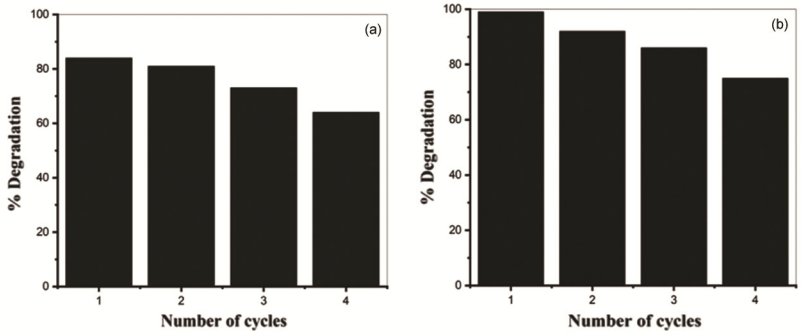

Fig. 13 — Reusability studies of (a) undoped and (b) Si-doped TiO_2-ZnO photocatalyst

Conclusion

Sol-gel method was used to successfully synthesize TiO_2-ZnO and Si-TiO_2-ZnO nanocatalysts. The synthesized catalysts were characterized and used for degradation of N-Nitrosomorpholine. The band gap of TiO_2-ZnO was found to be 3.2 eV, which decreased to 2.0 eV upon Si-doing, i.e. in Si- TiO_2-ZnO. The degradation of NMOR was effectively achieved by using 0.06 g of Si-TiO_2-ZnO catalyst, with a substrate concentration of 5 ppm, under the optimal conditions of sunlight, sonication and pH 4. The Si-TiO_2-ZnO catalyst exhibited superior NMOR degradation ability compared to the undoped TiO_2-ZnO catalyst. There is a slight reduction in the degradation efficiencies of both the catalysts even after 4th cycle. These materials also possessed remarkable inhibition activities in the antibacterial and antifungal studies.

Acknowledgement

The authors would like to thank Sophisticated Test and Instrumentation Centre (STIC), Cochin, Scudder Diagnostic Centre, Nagercoil, Karunya Institute of Technology and Sciences, Coimbatore, Instrumentation Centre Atta Nadar Janaki Ammal College, Sivakasi, Vels institute of technology, Chennai, Scott Christian College, Nagercoil for different characterisation techniques.

References

1 Subramaniam M N, Goh P S, Lau W J, Cheer N B & Ismail A F, Development of nanomaterial-based photocatalytic membrane for organic pollutants removal, *Adv Nanomater Membr Synth Appl*, (2019) 45.

2 Ferrari-Lima A M, Marques R G, Fernandes-Machado N R C, Gimenes M L, Photodegradation of sugarcane vinasse: evaluation of the effect of vinasse pre-treatment and the crystalline phase of TiO_2, *Catal Today*, 209 (2013) 79.

3 Suganthi N & Pushpanathan K, Photocatalytic degradation and antimicrobial activity of transition metal doped mesoporous ZnS nanoparticles, *Int J Environ Sci Technol*, 16 (2019) 3375.

4 Steinmetz K A & Potter J D, Vegetables, fruit, and cancer. II. Mechanisms, *Cancer Causes Contr*, 2 (1991) 427.

5 Tenovuo J, The biochemistry of nitrates, nitrites, nitrosamines and other potential carcinogens in human saliva, *Oral Pathol*, 15 (1986) 303.

6 Pegg A E, Determination of effects and binding properties of N-Nitrosomorpholine and N-Nitrosopyrrolydine on human acrosin by thin layer chromatography, *IARC Sci Publ*, 27 (1996) 3.

7 Brown J L, N-Nitrosamines, *Occup Med*, 14 (1999) 839.

8 Elmorsi T M, Riyad Y M, Mohamed Z H & Abd-El-Bary H M H, Decolorization of Mordant red 73 azo dye in water using H_2O_2/ UV and photo-Fenton treatment, *J Hazard Mater*, 174 (2010) 352.

9 Sharotri N & Sud D, A greener approach to synthesize visible light responsive nanoporous S-doped TiO_2 with enhanced photocatalytic activity, *New J Chem*, 39 (2015) 217.

10 Hamadanian M, Reisi-Vanani A & Majedi A, Synthesis, characterization and effect of calcination temperature on phase transformation and photocatalytic activity of Cu, S-codoped TiO_2 nanoparticles, *J Appl Surf Sci*, 256 (2010) 1837.

11 Al-Qaradawi S & Salman S R, Photocatalytic degradation of methyl orange as a model compound, *J Photochem Photobiol A: Chem*, 148 (2002) 161.

12 Ogawa H, Abe A, Nishikawa M & Hayakawa S, Preparation of tin oxide films from ultrafine particles, *J Electrochem Soc*, 128 (1981) 685.

13 Iqbal M N, Mesoporous silica particles for a potential therapeutic application, academic dissertation for the degree of Doctor of Philosophy in Materials Chemistry, Stockholm University, (2023).

14 Sapawe N & Hanafi M F, Facile one-pot electrosynthesis of high photoreactive hexacoordinated Si with Zr and Zn catalyst, RSC *Adv*, 5 (2015) 75141.

15 Sapawe N, Effective solar-based iron oxide supported HY zeolite catalyst for the decolorization of organic and simulated dyes, *New J Chem*, 39 (2015) 6377.

16 Sapawe N, Hybridization of zirconia, zinc and iron supported on HY zeolite as a solar-based catalyst for the rapid decolorization of various dyes, *New J Chem*, 39 (2015) 4526.

17 Sapawe N, Jaafar N F & Hairom N H H, Satar M A H, Ariffin M N, Triwahyono S & Jalil A A, A facile preparation of nanosized ZnO and its use in photocatalytic decolorization of methyl orange, *Malay J Fund Appl Sci*, 7 (2011) 19.

18 Sapawe N, Jalil A A & Triwahyono S, Photodecolorization of methylene blue over EGZrO2/HY in aqueous alkaline solution, *Malay J Fund Appl Sci*, 7 (2011) 137.